CHEMISTRY OF MATERIALS

ARTICLE

pubs.acs.org/cm

Synthesis, Dispersion, and Viscosity of Poly(ethylene glycol)-Functionalized Water-Soluble Single-Walled Carbon Nanotubes

Irina Kalinina,[†,‡] Kimberly Worsley,[†,‡] Christopher Lugo,[‡] Swadhin Mandal,[†,∥] Elena Bekyarova,[†,‡] and Robert C. Haddon*[,†,‡,§]

[†]Center for Nanoscale Science and Engineering, [‡]Department of Chemistry, and [§]Department of Chemical and Environmental Engineering, University of California, Riverside, California 92521, United States

Supporting Information

ABSTRACT: The carbon nanotube−polyethylene glycol (PEG) graft copolymer was synthesized by covalent functionalization of electric arc single-walled carbon nanotubes (SWNTs) with the monofunctional, tetrahydrofurfuryl-terminated polyethylene glycol PEG-THFF (MW∼200), to give a material composed of 80 wt % SWNTs. We show that the sequential processing of the resulting material by ultrasonication and high-shear mixing provides a means to disperse the SWNT-PEG-THFF macromolecules on two different length scales and leads to highly viscous solutions; at a concentration of 10 mg/mL the kinematic viscosity (ν) of an aqueous SWNT-PEG-THFF dispersion reaches a value of ν > 1000 cSt (for water ν ∼ 1 cSt). Analysis of this procedure by means of viscosity measurements and atomic force microscopy (AFM), shows that ultrasonication is effective in disrupting the SWNT bundles, while the high shear mixing disperses the individual SWNTs. The kinematic viscosity of aqueous dispersions of SWNT-PEG-THFF was measured as a function of nanotube concentration and compared to that of SWNT-PEG dispersions. The viscosity and AFM measurements show that the SWNT-PEG-THFF and SWNT-PEG graft copolymers form aqueous dispersions with distinct viscous characteristics; the use of monofunctional PEG-THFF for covalent functionalization of the SWNTs prevents cross-linking of the SWNTs in the final product, and this allows the production of more completely dispersed SWNTs than in the case of the SWNT-PEG graft copolymer, which is synthesized from a bifunctional glycol.

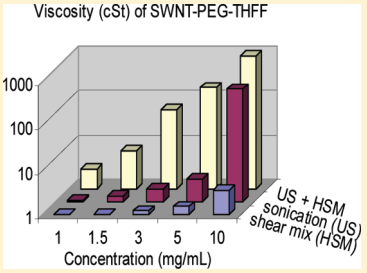

KEYWORDS: single-walled carbon nanotubes, covalent functionalization, polyethylene glycol, dispersion, kinematic viscosity

INTRODUCTION

The ability to process single-walled carbon nanotubes (SWNTs) is crucial for the translation of their excellent properties into functional materials and devices. This has been demonstrated in the development of composite materials,[1] the preparation of conductive and transparent thin films,[2,3] heat transfer systems,[4,5] and electronic devices and sensors.[6−10] Covalent functionalization has been widely used for the preparation of SWNT materials with select and improved dispersibility in solvents;[11−18] we have applied this technique to prepare a range of functionalized SWNTs[19−24] that have very good solubility in common organic solvents.

The functionalization of SWNTs with water-soluble polymers such as poly(*m*-aminobenzene sulfonic acid), PABS,[25] and polyethylene glycol (PEG)[23,26] have resulted in SWNT graft copolymers with high dispersibility in water. The covalent approach to the preparation of water-soluble SWNTs provides materials with controlled composition and reproducible properties, which is of significant importance for biomedical studies. This allowed studies, which utilize these materials as scaffolds for the nucleation of artificial bone material[27,28] and neuronal growth.[29−33]

Among the water-soluble polymers used for chemical modification of carbon nanotubes, PEG has received significant attention because of its biocompatibility. Non-covalent modification of carbon nanotubes with PEG has been shown to render them soluble in physiological buffers,[34] and these systems have been studied as molecular transporters inside mammalian cells,[35] as agents for selective probing and imaging of cells with fluorescence spectroscopy,[36] and tumor targeting agents.[37] In addition to the non-covalent approach,[34,38,39] ionic[40] and covalent chemistry[14,23,41,42] have been used to prepare SWNT−PEG derivatives. PEG of various molecular weights (MW) have been covalently attached to the carbon nanotubes: monoamine-terminated-PEG (MW = 5000),[41] diamine-terminated PEG (MW = 1500),[14,42] and PEG (MW = 600).[23]

In the present study we report the synthesis of a SWNT-PEG compound which is prepared by covalent attachment of a tetrahydrofurfuryl terminated PEG derivative to electric arc-produced SWNTs. This material differs from the previously reported SWNT-PEG material[23] by the fact that it utilizes monofunctional PEG, which prevents cross-linking between the nanotubes and as a result it enhances the dispersibility in water. The sequential application of ultrasonication and high-shear mixing of the SWNT-PEG-THFF in water gives dispersions of high

Received: October 21, 2010
Revised: December 16, 2010
Published: January 27, 2011

viscosity with substantially debundled carbon nanotubes. These dispersions appear to be stable over long period of time (months), and this may be due to intertube interactions, which prevent precipitation of the functionalized nanotubes. While highly viscous nanotubes dispersions may find application as heat transfer fluids, the primary outcome of the present work is the preparation of well dispersed aqueous SWNT solutions containing individual carbon nanotubes in the absence of surfactants.

EXPERIMENTAL SECTION

Materials. Purified electric arc produced SWNTs with carboxylic acid functionality (SWNT-COOH, P3-SWNT) were obtained from Carbon Solutions, Inc. (www.carbonsolution.com). Oxalyl chloride and tetrahydrofurfuryl polyethylene glycol (PEG-THFF, $C_5H_9O(C_2H_4O)_{n=2,3}OH$, MW∼200) were purchased from Sigma-Aldrich and anhydrous *N,N*-dimethylformamide (DMF) from EMD Chemicals, Inc. The functionalization reactions were performed under argon using oven-dried glassware.

SWNT-PEG-THFF Graft Copolymer. A 1 g portion of P3-SWNT material was dispersed in 1 L of anhydrous dimethylformamide (DMF) by ultrasonication for 2 h and high-shear mixing for 1 h to give a homogeneous suspension. Oxalyl chloride (20 mL) was added dropwise to the SWNT solution at 0 °C under argon. The reaction mixture was stirred at 0 °C for 1 h at room temperature for 2 h, followed by overnight heating at 70 °C to remove the excess oxalyl chloride (boiling point 63 °C). The functionalization was performed by addition of PEG-THFF (12 mL) at room temperature and the mixture was heated at 120 °C for 5 days. After cooling to room temperature the mixture was filtered through a 0.22-μm Teflon membrane, and washed with DMF and distilled water. The product was dried under vacuum to yield a black solid with a typical yield of 113%.

Characterization. Mid-IR spectra were measured using a Nicolet Nexus 670 FT-IR spectrometer at 8 cm^{-1} resolution in the frequency range 400−4,000 cm^{-1}; the samples were prepared from aqueous dispersions as thin films on ZnSe substrates. Raman spectra were collected using a Nicolet Almega XR Raman microscope with laser excitation of 532 nm.

Solubility Test. The solubility in water was estimated using a previously reported procedure.[23] Briefly, 100 mg of the material was dispersed in 10 mL of distilled water by ultrasonication for 4 h and left to stand overnight. An aliquot of 50 μL was diluted to 25 mL, and the concentration of the solution was estimated from the absorption intensity at 550 nm and the extinction coefficient of the material (ε = 19.2 L cm^{-1} g^{-1}, Supporting Information).

Dispersion of SWNT materials. The SWNT-PEG-THFF and SWNT-PEG materials were dispersed in distilled water using different techniques: high shear-mixing (HSM), ultrasonication (US), and a combination of ultrasonication and high shear-mixing (US + HSM). Dispersions with concentrations in the range of 1 to 10 mg/mL were prepared in 25 mL of water. The ultrasonication was performed in a bath sonicator (Aquasonic 50HT, VWR Scientific, sonic power 75 W, frequency ∼40 kHz) for 20 h. It has been suggested that extensive sonication may induce defects in the nanotube structure and even lead to mechanical damage.[43−45] We used Raman spectroscopy to estimate the effect of prolonged ultrasonication on the quality of the SWNT material. Figure 1 compares the Raman spectra of SWNT-PEG-THFF before and after dispersion processing; for the sonicated material the spectra were taken on films prepared by filtration of the dispersions. It is apparent that after processing the intensity of the D-band observed at 1342 cm^{-1}, which is associated with defects,[46] remains very small compared to the G-band intensity. It should be noted that the effect of the sonication on the nanotube structure depends on the sonication energy and frequency and the solvent media;[43] the damage of nanotubes during sonication is expected to be minimized when water is used as a medium because of the efficiency of the cavitation energy transfer.[43]

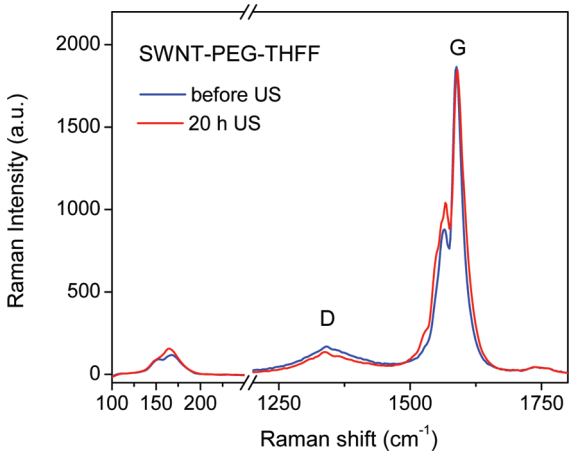

Figure 1. Raman spectra (λ_{EX} = 532 nm) of SWNT-PEG-THFF material before (blue line) and after (red line) ultrasonication (US) for 20 h. The spectra are normalized to the intensity of the G-band.

The high-shear mixing of the dispersions was performed for 1 h with a homogenizer (Fisher TissueMixer, motor speed of 30,000 rpm). In the sequential dispersion processing, the nanotube dispersions were first ultrasonicated for 20 h and then high-shear mixed for 1 h.

Viscosity Measurements. The kinematic viscosity of the aqueous dispersions of nanotubes was measured using Fisherbrand Glass Ubbelohde Calibrated Viscometer Tubes, ASTM sizes 1C, 2, 2B, and 3C; this set of tubes allowed to measure the viscosity of a series of dispersions in the range 6 to 3,000 cSt. The viscometer size for each measurement was selected to allow a flow time of at least 100 s. The dispersions were introduced into the viscometer using a pipet. The viscometer was kept at room temperature until it reached thermal equilibrium. Efflux time was measured by allowing the sample to flow freely through the capillary of the viscometer, and the measurement was repeated five times (readings within 0.1%) to obtain an average value of the kinematic viscosity. To calculate the kinematic viscosity in cSt (mm^2/s), the efflux time in seconds was multiplied by the viscometer constant, c [c = 0.03047 (size 1c), c = 0.09616 (size 2), c = 0.5098 (size 2B), and c = 2.888 (size 3C)].

Diameter and Length Distribution Analysis. The distribution curves were obtained from a statistical analysis of the atomic force microscopy (AFM) images; the samples for AFM analysis were prepared from diluted dispersions of the materials, which were dropped on a mica substrate and the images were recorded in tapping mode with a Digital Instruments Nanoscope IIIA using a n^+-silicon cantilever with a force constant of 40 N m^{-1}. Five images (10 μm × 10 μm) at different locations on the mica substrate were recorded for each dispersion. The AFM J scanner was calibrated using a 3D reference (Veeco, P/N 498−000−026) with a 10 μm lateral pitch and a step height of 100 nm. The SWNT diameter was determined from the AFM height measurements. A minimum of 100 tubes were measured for each of the statistical analyses.

RESULTS AND DISCUSSION

1. Synthesis and Product Characterization. We previously reported that the covalent attachment of polyethylene glycol (PEG, MW = 600) to SWNTs led to a graft copolymer with high solubility in water (∼6 g/L).[23] Here we use PEG-THFF, which is a monofunctional oligomer with a tetrahydrofurfuryl termination as opposed to the bifunctional PEG; thus, we anticipated that the

Scheme 1. Schematic Illustration of the Functionalization of SWNTs with PEG-THFF

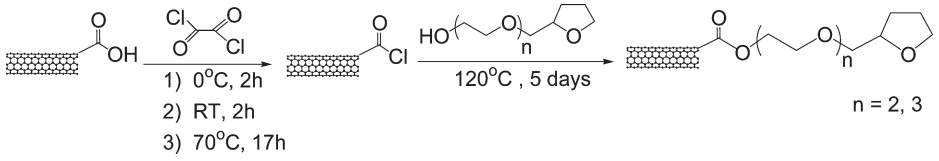

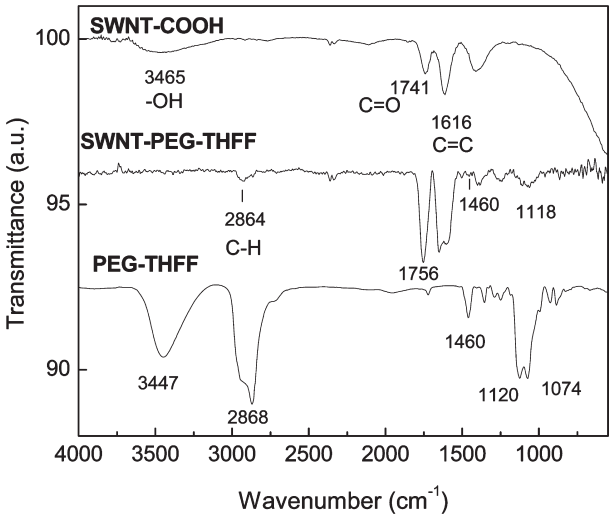

Figure 2. FT-IR spectra of films of SWNT-COOH, PEG-THFF, and SWNT-PEG-THFF deposited on ZnSe.

use of this reagent would prevent cross-linking between the nanotubes and therefore enhance the processability of the SWNT-PEG-THFF graft copolymer. In addition, the PEG-THFF used in the present procedure has a very short chain (MW∼200), and this has the potential for increased SWNT content in the final graft copolymer. For the synthesis, the carboxylic acid groups in purified SWNTs were converted to acyl chloride and subsequently reacted with the PEG-THFF to obtain the final product, SWNT-PEG-THFF (Scheme 1).[23]

The covalent functionalization, which occurs through the formation of an ester bond between the nanotubes and PEG chain, was confirmed by mid-IR spectroscopy. Figure 2 compares the FT-IR spectra of PEG-THFF, SWNT-COOH, and SWNT-PEG-THFF. The IR spectrum of the SWNT-COOH starting material shows a broad peak at 1741 cm^{-1}, which is assigned to the C═O stretching vibration of the carboxylic acid groups[11,21] and the peak centered at 1616 cm^{-1} is in the region of vibrations previously assigned to localized C═C bonds or conjugated carbonyl or carboxylic acid groups.[47−49] In the spectra of the SWNT-PEG-THFF graft copolymer the C═O stretch is shifted to 1756 cm^{-1}, because of the formation of an ester bond[23] (Scheme 1), and the OH stretching vibration, which appears at 3447 cm^{-1} in the spectrum of PEG-THFF, is not present. The broad peaks, centered at 2868 cm^{-1} (PEG-THFF) and 2864 cm^{-1} (SWNT-PEG-THFF), arise from the C−H stretching vibrations. The deformation vibration of the CH_2 group gives a peak at 1460 cm^{-1}, which in the spectra of neat PEG-THFF overlaps with the OH-deformation vibration, and the C−O stretching vibration of the ethers appears in the vicinity of 1100 cm^{-1}.

Using TGA and near-IR spectroscopy we estimated that the SWNT-PEG-THFF material contains ∼82 wt % SWNTs (Supporting Information). On the basis of the weight percentage of SWNTs in the functionalized material and the molecular weight of PEG-THFF (MW = 200), we calculate that the fraction of carbon atoms in the SWNTs, which participate in covalent bond formation with PEG-THFF, is 1.3 mol %: (18/200)/(82/12) × 100. For comparison, in the previously synthesized SWNT-PEG graft copolymer[23] about 1 mol % of the SWNT C-atoms react with the PEG-moieties.

The content of PEG-THFF in the graft copolymer depends on the concentration of carboxylic acid groups in the starting SWNT material (SWNT-COOH) and the degree of completion of the reaction. We determined the concentration of the carboxylic acid groups in the SWNT-COOH starting material by acid−base titration[50] (Supporting Information). In this procedure the forward titration determines the total acid groups present in the starting material and together with the SWNT-COOH functionality it includes residual intercalated acid from the purification process[51] and carboxylic acid-functionalized carbonaceous impurities.[22,24,52−54] The latter two impurity components are washed away before the back-titration which determines the acid content in just the SWNT-COOH fraction, and it is important to note that our synthetic procedure partly removes the functionalized carbonaceous impurities.[24,53−55] Thus, in comparing the degree of functionalization of the SWNT-COOH starting material, we adopt the figure from the back-titration, which gives 1.3 mol % carboxylic acid groups. (Supporting Information) From this analysis we conclude that the current procedure allows for almost complete reaction between the carboxylic groups in the SWNTs and the PEG-THFF.

The SWNT-PEG-THFF material exhibits high solubility in water (9.2 mg/mL), and during the solubility tests it was observed that prolonged ultrasonication of concentrated aqueous dispersions of SWNT-PEG-THFF resulted in the formation of extremely viscous dispersions. This prompted us to study the viscosity of the SWNT-PEG-THFF dispersions and compare their visco-elastic properties with those of SWNT-PEG dispersions.

2. Viscosity Measurement. The kinematic viscosity (ν), which is the absolute or dynamic viscosity (η) divided by the density (ρ), was measured to compare the aqueous dispersions of two different PEG- functionalized SWNT materials, SWNT-PEG-THFF ($MW_{PEG\text{-}THFF}$ = 200) and SWNT-PEG (MW_{PEG} = 2600).[23] Aqueous dispersions with a concentration of 5 mg/mL were prepared by ultrasonication for 20 h. The measured kinematic viscosity (ν) of the SWNT-PEG-THFF dispersion was ν = 3.3 cSt, while the SWNT-PEG dispersion showed two times lower viscosity, ν = 1.6 cSt. As the nominal concentration increases to 10 mg/mL the SWNT- PEG-THFF forms dispersions, which are 2 orders of magnitude higher in viscosity (ν = 339 cSt) in comparison to SWNT-PEG dispersions (ν = 3.58 cSt).

Because the viscosity is sensitive to the degree of exfoliation of SWNTs,[56] we explored different techniques to debundle the SWNT materials and compared their kinematic viscosities (ν) as a function of materials concentration. In addition to ultrasonication

dx.doi.org/10.1021/cm103030s |Chem. Mater. 2011, 23, 1246–1253

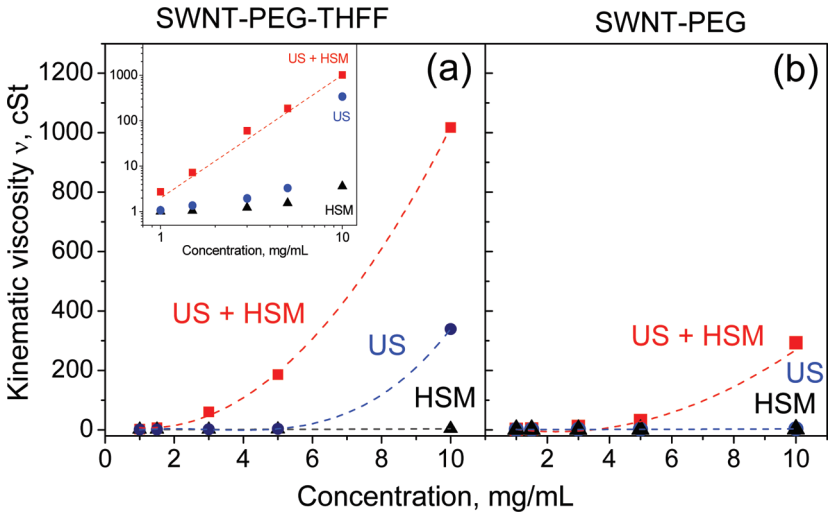

Figure 3. Kinematic viscosity (ν) as a function of concentration of aqueous dispersions of (a) SWNT-PEG-THFF and (b) SWNT-PEG, prepared by 20 h ultrasonication (US), 1 h high shear mixing (HSM), and a combination of 20 h ultrasonication and 1 h high shear mixing (US + HSM). The inset in panel (a) shows a log−log plot of the experimental data.

(US) for 20 h, we used high shear-mixing (HSM) for 1 h and a combination of ultrasonication and high shear-mixing (US+HSM, 20 h ultrasonication followed by 1 h HSM). These three techniques were used to prepare aqueous dispersions of SWNT-PEG-THFF and SWNT-PEG with concentrations in the range of 1 mg/mL−10 mg/mL. The measured kinematic viscosity (ν) in Figure 3 shows the effectiveness of the three techniques in dispersing the SWNT-PEG materials.

High shear-mixing (HSM) alone is apparently not efficient in dispersing the SWNT materials and produces dispersions with visible aggregates and very low viscosity; even at 10 mg/mL the kinematic viscosity of SWNT-PEG-THFF is only ν = 3.6 cSt, whereas for SWNT-PEG ν = 1.2 cSt [close to the viscosity of the solvent (water)]. The viscosity of the dispersions shows linear dependence on concentration over the whole range of concentrations (1 to 10 mg/mL).

Ultrasonication (US) of the two types of PEG-functionalized SWNT materials in water for 20 h resulted in homogeneous dispersions without visual aggregates. The viscosity measurements revealed different behavior for the two materials: the viscosity of the SWNT-PEG dispersions shows a linear increase with concentration over the whole concentration range, whereas the viscosity of the SWNT-PEG-THFF dispersions follows a slow linear increase until 5 mg/mL followed by an abrupt increase in viscosity at 10 mg/mL. This may be due to the higher dispersibility of SWNT-PEG-THFF, which results in higher effective concentration of SWNTs in the dispersion.

The sequential combination of the two methods, ultrasonication and high shear-mixing (US+HSM), was found to have a synergistic effect on the viscosity of both materials. At 10 mg/mL the viscosity of the SWNT-PEG-THFF dispersions reaches ν = 1018 cSt, which is ~300 times higher than the viscosity of dispersions prepared by high shear-mixing and 3 times higher than the viscosity of dispersions, prepared by the ultrasonication method. For the SWNT-PEG material, this method provides dispersions with higher viscosity at concentrations above 5 mg/mL, although the viscosities of the dispersions are significantly lower than those of SWNT-PEG-THFF. Thus, the viscosity measurements indicate that the combination of sonication and high-shear mixing is an effective technique for dispersing SWNT materials.

In terms of visco-elastic behavior carbon nanotube dispersions are generally treated as polymer solutions.[57−59] In a dilute solution the individual macromolecules (polymer or carbon nanotube) can be considered independent or non-interacting, and their Brownian motion is determined by the viscosity of the solvent. The linear dependence of the viscosity on concentration suggests the absence of interactions between the dispersed SWNT objects and incomplete SWNT exfoliation; such behavior is observed for dispersions of both materials prepared by high-shear mixing and for the sonicated dispersions of SWNT-PEG.

In concentrated solutions or dispersions, intermolecular interactions and entanglement suppress the free rotational and translational motions of the particles[57] and at the entanglement concentration (also known as critical concentration, C_C), which is related to the hydrodynamic volume of the particles, the viscosity of the nanotube dispersion dramatically increases.[60] In this concentration range the viscosity becomes strongly dependent on the concentration (C) and the aspect ratio (L/D) of the dispersed objects, and it can be described by the equation $\eta_{sp} \approx C^3(L/D)^6/\ln(L/D)$, where the absolute or dynamic viscosity (symbolized by μ or η) is the product of the density (ρ) and the kinematic viscosity (ν), $\eta = \rho\nu$, and the specific viscosity is given by $\eta_{sp} = (\eta - \eta_0)/\eta_0$, where η_0 is the dynamic viscosity of the solvent.[56] This equation was fitted to the viscosity of SWNT-PEG-THFF dispersions, prepared by the sequential dispersal method (US+HSM), and as shown in the inset of Figure 3a the data fits the model over the whole concentration range; the inset of Figure 3a clearly shows a power law dependence on the concentration with a slope of 3. In contrast, the dispersions of SWNT-PEG-THFF, prepared by ultrasonication, showed an almost linear dependence on concentration (C < 5 mg/mL). The differences in the dependence of the viscosity on concentration for dispersions prepared by the two techniques, suggest that they give rise to distinct levels of SWNT exfoliation.

To further examine the exfoliation process we used atomic force microscopy to analyze the nanotube length and diameter distributions in the SWNT-PEG-THFF dispersions; the exfoliation of the SWNT bundles is expected to increase the aspect ratio of the dispersed nanotubes. The AFM measurements showed

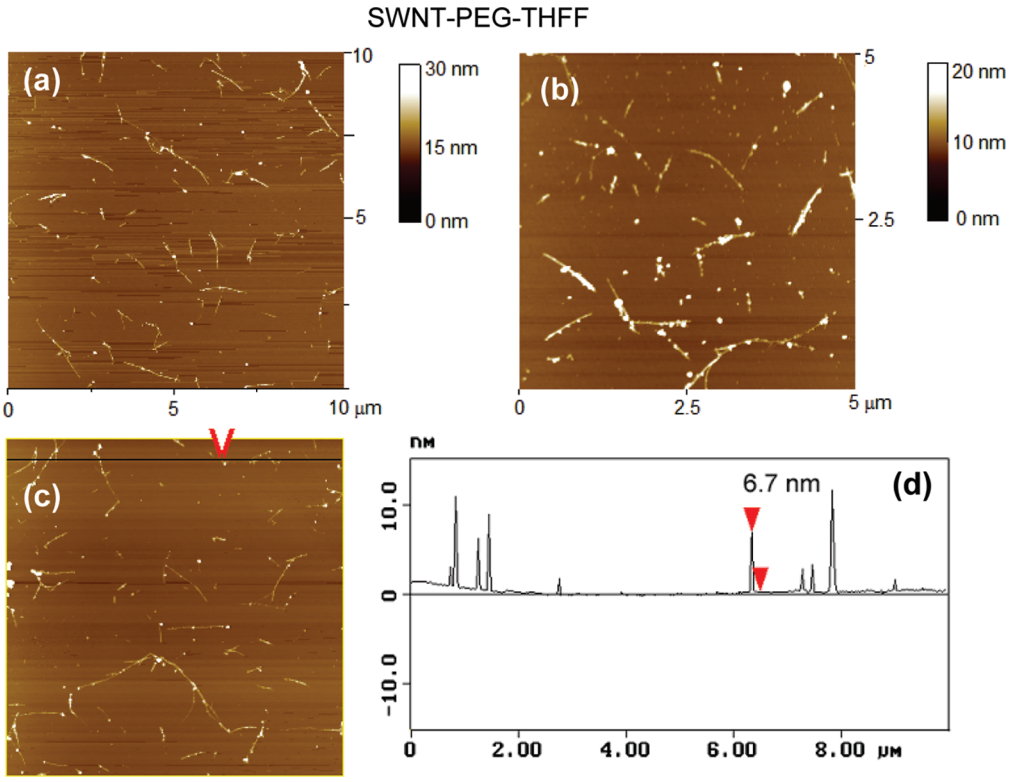

Figure 4. (a−c) AFM images of SWNT-PEG-THFF samples obtained from ultrasonicated aqueous dispersions. (d) Height analysis.

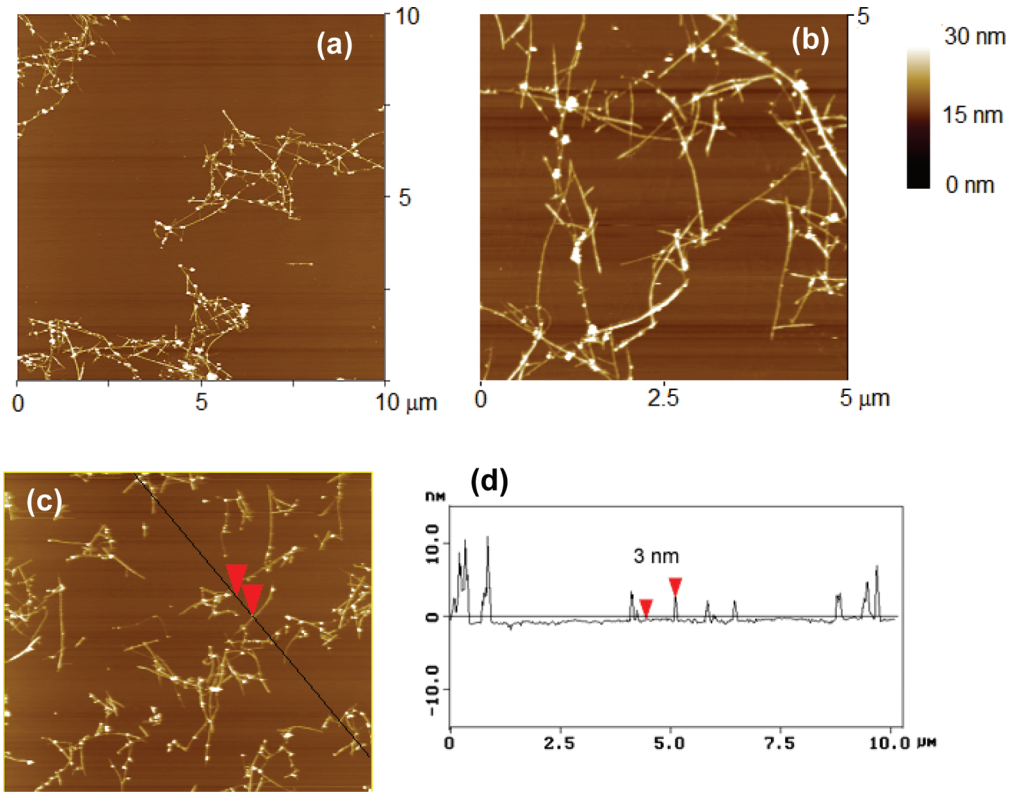

Figure 5. (a−c) AFM images of SWNT-PEG samples obtained from ultrasonicated aqueous dispersions. (d) Height analysis.

that both length and diameter of the SWNT-PEG-THFF present in the aqueous dispersions were affected by the dispersion procedure.

Figure 4 shows representative AFM images of SWNT-PEG-THFF as it is present in dispersions ultrasonicated for 20 h.

dx.doi.org/10.1021/cm103030s |*Chem. Mater.* 2011, 23, 1246–1253

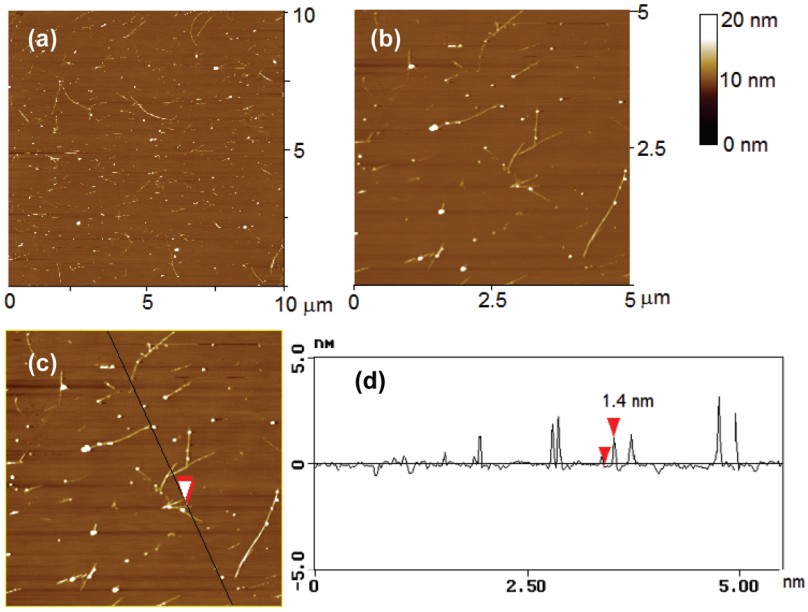

Figure 6. AFM images of aqueous dispersions of SWNT-PEG-THFF prepared by sequential processing using sonication and high-shear mixing. (d) Height analysis of functionalized nanotubes.

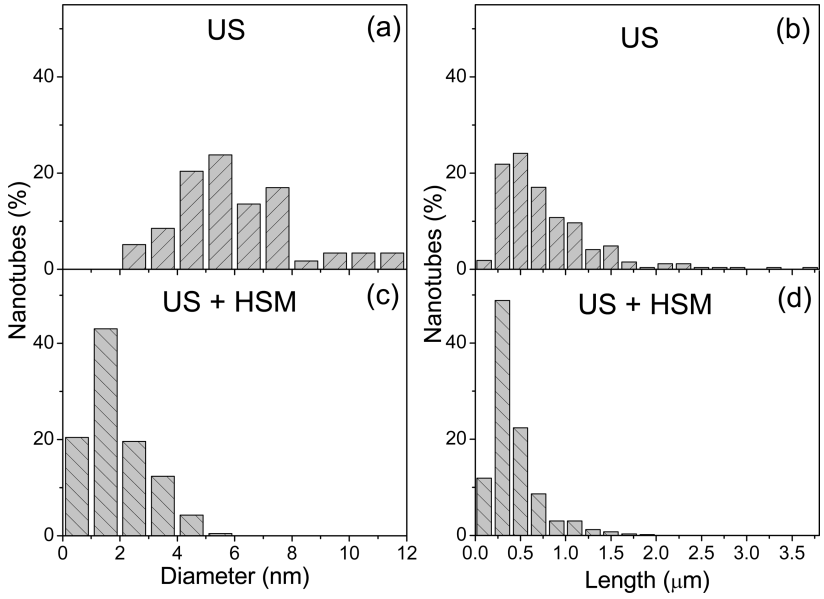

Figure 7. Normalized Diameter and length distributions of the SWNT-PEG-THFF material obtained from AFM analysis. Dispersions formed by (a, b) ultrasonication and (c,d) ultrasonication followed by high shear-mixing.

Usually the functionalized SWNTs exist in small bundles with a relatively broad range of diameter and length distributions.

However, in the ultrasonicated dispersions of the SWNT-PEG material (Figure 5), the nanotubes are interconnected to form clusters or aggregates, which vary in size and often exceed 5 μm in size. We associate the formation of these clusters with nanotube cross-linking that occurs during the reaction with the bifunctional PEG. Thus, we anticipate that the difference in the viscosities of the dispersions of SWNT-PEG-THFF and SWNT-PEG is partly due to morphological differences as a result of opportunities for chemical cross-linking of the SWNTs in the latter material.

Similar AFM images (Supporting Information, Figure SI3) were obtained for dispersions prepared by sequential processing of the SWNT-PEG material with ultrasonication and then high-shear mixing.

The combination of sonication for 20 h and high-shear mixing for 1 h, resulted in efficient exfoliation of the SWNT-PEG-THFF samples with a large fraction of individual nanotubes and small bundles (Figure 6).

Statistical analysis of the AFM images of the SWNT-PEG-THFF material is presented in Figure 7; analysis of the SWNT-PEG dispersions was not performed because of the cross-linking of the PEG-functionalized nanotubes. The ultrasonicated dispersions of SWNT-PEG-THFF have a broad diameter distribution with large bundles and a small percentage of small bundles and individual tubes; the average diameter of the bundles is

dx.doi.org/10.1021/cm103030s |*Chem. Mater.* 2011, 23, 1246–1253

Table 1. Morphological Characterization of SWNT-PEG-THFF Partly Debundled by Ultrasonication and Fully Exfoliated by a Combination of Ultrasonication and High-Shear Mixing

dispersion method	mean diameter, D μm	mean length, L μm	L/D	critical conc. vol %
ultrasonication	6×10^{-3}	0.6	100	0.015
ultrasonication +high-shear mixing	2×10^{-3}	0.4	200	0.004

Scheme 2. Schematic Illustration of the Mechanisms of Dispersion of the Functionalized SWNTs by Sonication and High Shear Mixing

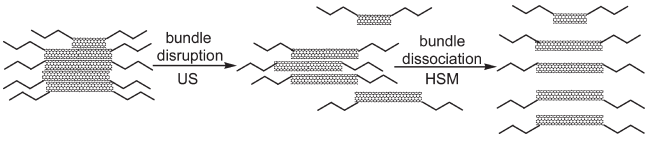

~6 nm and average length is ~600 nm (Figure 7a,b). The application of ultrasonication followed by high-shear mixing achieved a much more complete debundling of the nanotubes; statistical analysis of the AFM data showed an average SWNT diameter of ~1.5 nm and indicated that more than 65% of the nanotubes were present as individual SWNTs or very small bundles (Figure 7c).

In addition, the AFM analysis shows a reduced length of the SWNT-PEG-THFF with the majority of the nanotubes in the range of ~400 nm (Figure 7d); the reduced length of the nanotubes is ascribed to the exfoliation of bundles composed of short nanotubes.

On the basis of the data from the AFM analysis we calculated the critical concentration of SWNTs (Table 1), that is, the concentration below which the dispersed nanotubes do not interact with each other and can rotate freely (for this calculation the number of nanotubes, which do not interact, is estimated by assuming that the nanotube hydrodynamic diameter is given by the average nanotube length). For the dispersions prepared by ultrasonication we obtain a critical concentration, C_C = 0.015 vol %, and thus the concentration of the dispersions reported herein (10 mg/mL or 0.8 vol % assuming a SWNT density of 1.2 g/mL) exceeds the critical concentration by a factor of more than 50. In the case of the highly exfoliated nanotube dispersions, prepared by a combination of ultrasonication and high-shear mixing, C_C = 0.004 vol %, and the dispersions exceed the critical concentration by a factor of 220. Previous studies have reported critical concentrations of C_C = 0.7 vol %[60] and C_C = 0.5 vol %[59] for oxidized MWNTs dispersed in water. We ascribe the very low critical concentrations and high viscosities of the dispersions reported in our study to the high level of nanotube exfoliation.

The viscosity and AFM analyses confirm that the sequential application of ultrasonication and high shear mixing is much more effective in exfoliating the SWNT-PEG-THFF than other combinations of these procedures; the reverse procedure (high-shear mixing followed by ultrasonication) did not give viscous dispersions, and this shows that the sequence in which the two techniques are used is essential for efficient nanotube exfoliation. This behavior can be understood in the light of the different length and energy scales over which sonication and shear mixing act on the bundled nanotubes,[4,45,61−64] and bears an obvious resemblance to the unzipping mechanism previously advanced to understand the dispersion of carbon nanotubes in the presence of surfactants.[62]

During bath ultrasonication the acoustic waves nucleate bubbles at the surface of nanotubes (bundles) which then collapse; cavitation due to the highly anisotropic localized implosion of the bubbles fractures the nanotube aggregates and frays the ends of the nanotube bundles because of the nonuniform flow field;[45] these shear forces are due to localized fluid friction at the nanotube surface and may not lead to complete dispersal of individual nanotubes. However, the shear forces generated in the high shear mixing process are uniform across a large volume of the solvent and thus they act at a larger length scale thereby applying a shear force across the whole (frayed) nanotube bundle, and this allows the full separation of individual nanotubes (Scheme 2). The hydrodynamic stress on the small nanotube bundles (partially exfoliated by the ultrasonication and intercalated with solvent molecules and the PEG-THFF chain) is strong enough to overcome the remaining attachment between the nanotubes. Thus, beginning the dispersion process with high shear mixing of the SWNT material is not effective in exfoliating the nanotube bundles because there is insufficient localized energy to begin the disruption of the intact nanotube bundles.

CONCLUSIONS

We report the preparation of a SWNT-PEG derivative with very high solubility in water (~9 g/L). Because the covalently attached ethylene glycol oligomer is short (MW~200), the SWNT-PEG-THFF graft copolymer consists of more than 80 wt % SWNTs. Despite the high SWNT loading, the material forms stable dispersions in water at high concentrations. The functionalized SWNTs are efficiently debundled by a combination of ultrasonication and high-shear mixing in aqueous media, and this affords dispersions of extremely high viscosity. We found that the exponential increase of viscosity with concentration is due to the high aspect ratio of the exfoliated SWNTs.

ASSOCIATED CONTENT

Supporting Information. Additional characterization data from TGA, acid−base titration, extinction coefficient, and AFM. This material is available free of charge via the Internet at http://pubs.acs.org.

AUTHOR INFORMATION

Corresponding Author

*E-mail: haddon@ucr.edu.

Current Address

[||]Department of Chemical Sciences, Indian Institute of Science Education and Research-Kolkata, Mohanpur-741252, India.

ACKNOWLEDGMENT

This material is based on research sponsored by DARPA/Defense Microelectronics Activity (DMEA) under agreement number H94003-10-2-1004.

REFERENCES

(1) Gao, J. B.; Itkis, M. E.; Yu, A.; Bekyarova, E.; Zhao, B.; Haddon, R. C. *J. Am. Chem. Soc.* **2005**, *127*, 3847–3854.

(2) Bekyarova, E.; Itkis, M. E.; Cabrera, N.; Zhao, B.; Yu, A.; Gao, J.; Haddon, R. C. *J. Am. Chem. Soc.* **2005**, *127*, 5990–5995.
(3) Gruner, G. *J. Mater. Chem.* **2006**, *16*, 3533–3539.
(4) Garg, P.; Alvarado, J. L.; Marsh, C.; Carlson, T. A.; Kessler, D. A.; Annamalai, K. *Int. J. Heat Mass Transfer* **2009**, *52*, 5090–5101.
(5) Nanda, J.; Maranville, C.; Bollin, C. M.; Sawall, D.; Ohtani, H.; Remillard, J. T.; Ginder, J. M. *J. Phys. Chem. C* **2007**, *112*, 654–658.
(6) Baughman, R. H.; Zakhidov, A. A.; Heer, W. A. *Science* **2002**, *297*, 787–792.
(7) Bekyarova, E.; Davis, M.; Burch, T.; Itkis, M. E.; Zhao, B.; Sunshine, S.; Haddon, R. C. *J. Phys. Chem. B* **2004**, *108*, 19717–19720.
(8) Meitl, M. A.; Zhou, Y.; Gaur, A.; Jeon, S.; Usrey, M. L.; Strano, M. S.; Rogers, J. A. *Nano Lett.* **2004**, *4*, 1643–1647.
(9) Bekyarova, E.; Kalinina, I.; Sun, X.; Shastry, T.; Worsley, K.; Chi, X.; Itkis, M. E.; Haddon, R. C. *Adv. Mater.* **2010**, *22*, 848–852.
(10) Ziegler, K. J. *Trends Biotechnol.* **2005**, *23*, 440–444.
(11) Chen, J.; Hamon, M. A.; Hu, H.; Chen, Y.; Rao, A. M.; Eklund, P. C.; Haddon, R. C. *Science* **1998**, *282*, 95–98.
(12) Bahr, J. L.; Yang, J.; Kosynkin, D. V.; Bronikowski, M. J.; Smalley, R. E.; Tour, J. M. *J. Am. Chem. Soc.* **2001**, *123*, 6536–6542.
(13) Sun, Y. P.; Fu, K.; Huang, W. *Acc. Chem. Res.* **2002**, *35*, 1096–1104.
(14) Chattopadhyay, J.; de Jesus Cortez, F.; Chakraborty, S.; Slater, N. K. H.; Billups, W. E. *Chem. Mater.* **2006**, *18*, 5864–5868.
(15) Tasis, D.; Tagmatarchis, N.; Bianco, A.; Prato, M. *Chem. Rev.* **2006**, *106*, 1105–1136.
(16) Strano, M. S.; Boghossian, A. A.; Kim, W. J.; Barone, P. W.; Jeng, E. S.; Heller, D. A.; Nair, N.; Jin, H.; Sharma, R.; Lee, C. Y. *MRS Bull.* **2009**, *34*, 950–961.
(17) Kahn, M. G. C.; Banerjee, S.; Wong, S. S. *Nano Lett.* **2002**, *2*, 1215–1218.
(18) Hirsch, A. *Angew. Chem., Int. Ed.* **2002**, *41*, 1853–1859.
(19) Chen, J.; Rao, A. M.; Lyuksyutov, S.; Itkis, M. E.; Hamon, M. A.; Hu, H.; Cohn, R. W.; Eklund, P. W.; Colbert, D. T.; Smalley, R. E.; Haddon, R. C. *J. Phys. Chem. B* **2001**, *105*, 2525–2528.
(20) Niyogi, S.; Hamon, M. A.; Hu, H.; Zhao, B.; Bhowmik, P.; Sen, R.; Itkis, M. E.; Haddon, R. C. *Acc. Chem. Res.* **2002**, *35*, 1105–1113.
(21) Hamon, M. A.; Chen, J.; Hu, H.; Chen, Y.; Itkis, M. E.; Rao, A. M.; Eklund, P. C.; Haddon, R. C. *Adv. Mater.* **1999**, *11*, 834–840.
(22) Hamon, M. A.; Hu, H.; Bhowmik, P.; Itkis, M. E.; Haddon, R. C. *Appl. Phys. A: Mater. Sci. Process.* **2002**, *74*, 333–338.
(23) Zhao, B.; Hu, H.; Perea, D.; Haddon, R. C. *J. Am. Chem. Soc.* **2005**, *127*, 8197–8203.
(24) Worsley, K. A.; Kalinina, I.; Bekyarova, E.; Haddon, R. C. *J. Am. Chem. Soc.* **2009**, *131*, 18153–18158.
(25) Zhao, B.; Hu, H.; Haddon, R. C. *Adv. Funct. Mater.* **2004**, *14*, 71–76.
(26) Riggs, J. E.; Guo, Z.-X.; Carroll, D. L.; Sun, Y. P. *J. Am. Chem. Soc.* **2000**, *122*, 5879–5880.
(27) Zhao, B.; Hu, H.; Mandal, S. K.; Haddon, R. C. *Chem. Mater.* **2005**, *17*, 3235–3241.
(28) Zanello, L. P.; Zhao, B.; Hu, H.; Haddon, R. C. *Nano Lett.* **2006**, *6*, 562–567.
(29) Hu, H.; Ni, Y.; Montana, V.; Haddon, R. C.; Parpura, V. *Nano Lett.* **2004**, *4*, 507–511.
(30) Hu, H.; Ni, Y.; Mandal, S. K.; Montana, V.; Zhao, B.; Haddon, R. C.; Parpura, V. *J. Phys. Chem. B* **2005**, *109*, 4285–4289.
(31) Ni, Y.; Hu, H.; Malarkey, E. B.; Zhao, B.; Montana, V.; Haddon, R. C.; Parpura, V. *J. Nanosci. Nanotechnol.* **2005**, *5*, 1707–1712.
(32) Malarkey, E. B.; Reyes, R. C.; Zhao, B.; Haddon, R. C.; Parpura, V. *Nano Lett.* **2008**, *8*, 3538–3542.
(33) Malarkey, E. B.; Fisher, K. A.; Bekyarova, E.; Liu, W.; Haddon, R. C.; Parpura, V. *Nano Lett.* **2009**, *9*, 264–268.
(34) Nakayama-Ratchford, N.; Bangsaruntip, S.; Sun, X. M.; Welsher, K.; Dai, H. J. *J. Am. Chem. Soc.* **2007**, *129*, 2448–2449.
(35) Kam, N. W. S.; Liu, Z.; Dai, H. J. *J. Am. Chem. Soc.* **2005**, *127*, 12492–12493.
(36) Welsher, K.; Liu, Z.; Daranciang, D.; Dai, H. *Nano Lett.* **2008**, *8*, 586–590.
(37) Schipper, M. L.; Nakayama-Ratchford, N.; Davis, C. R.; Kam, N. W. S.; Chu, P.; Liu, Z.; Sun, X.; Dai, H.; Gambhir, S. S. *Nat. Nanotechnol.* **2008**, *3*, 216–221.
(38) Chen, R. J.; Zhang, Y.; Wang, D.; Dai, H. *J. Am. Chem. Soc.* **2001**, *123*, 3838–3839.
(39) Zhang, F.; Zhang, H.; Zhang, Z.; Chen, Z.; Xu, Q. *Macromolecules* **2008**, *41*, 4519–4523.
(40) Huang, W. J.; Fernando, S.; Lin, Y.; Zhou, B.; Allard, L. F.; Sun, Y. P. *Langmuir* **2003**, *19*, 7084–7088.
(41) Sano, M.; Kamino, A.; Okamura, J.; Shinkai, S. *Langmuir* **2001**, *17*, 5125–5128.
(42) Huang, W. J.; Fernando, S.; Allard, L. F.; Sun, Y. P. *Nano Lett.* **2003**, *3*, 565–568.
(43) Lu, K. L.; Lago, R. M.; Chen, Y. K.; Green, M. L. H.; Harris, P. J. F.; Tsang, S. C. *Carbon* **1996**, *34*, 814–816.
(44) Niyogi, S.; Hamon, M. A.; Perea, D.; Kang, C. B.; Zhao, B.; Pal, S. K.; Wyant, A. E.; Itkis, M. E.; Haddon, R. C. *J. Phys. Chem. B* **2003**, *107*, 8799–8804.
(45) Lucas, A.; Zakri, C.; Maugey, M.; Pasquali, M.; Van der Schoot, P.; Poulin, P. *J. Phys. Chem. C.* **2009**, *113*, 20599–20605.
(46) Dresselhaus, M. S.; Jorio, A.; Hofmann, M.; Dresselhaus, G.; Saito, R. *Nano Lett.* **2010**, *10*, 751–758.
(47) Kuznetsova, A.; Mawhinney, D. B.; Naumenko, V.; Yates, J. T., Jr.; Liu, J.; Smalley, R. E. *Chem. Phys. Lett.* **2000**, *321*, 292–296.
(48) Kuznetsova, A.; Popova, I.; Yates, J. T.; Bronikowski, M. J.; Huffman, C. B.; Liu, J.; Smalley, R. E.; Hwu, H. H.; Chen, J. G. *J. Am. Chem. Soc.* **2001**, *123*, 10699–10704.
(49) Kim, U. J.; Furtado, C. A.; Liu, X. M.; Chen, G. G.; Eklund, P. C. *J. Am. Chem. Soc.* **2005**, *127*, 15437–15445.
(50) Hu, H.; Bhowmik, P.; Zhao, B.; Hamon, M. A.; Itkis, M. E.; Haddon, R. C. *Chem. Phys. Lett.* **2001**, *345*, 25–28.
(51) Itkis, M. E.; Niyogi, S.; Meng, M.; Hamon, M.; Hu, H.; Haddon, R. C. *Nano Lett.* **2002**, *2*, 155–159.
(52) Hamon, M. A.; Hu, H.; Bhowmik, P.; Niyogi, S.; Zhao, B.; Itkis, M. E.; Haddon, R. C. *Chem. Phys. Lett.* **2001**, *347*, 8–12.
(53) Niyogi, S.; Hu, H.; Hamon, M. A.; Bhowmik, P.; Zhao, B.; Rozenzhak, S. M.; Chen, J.; Itkis, M. E.; Meier, M. S.; Haddon, R. C. *J. Am. Chem. Soc.* **2001**, *123*, 733–734.
(54) Zhao, B.; Hu, H.; Niyogi, S.; Itkis, M. E.; Hamon, M.; Bhowmik, P.; Meier, M. S.; Haddon, R. C. *J. Am. Chem. Soc.* **2001**, *123*, 11673–11677.
(55) Haddon, R. C.; Sippel, J.; Rinzler, A. G.; Papadimitrakopoulos, F. *MRS Bull.* **2004**, *29*, 252–259.
(56) Cotiuga, I.; Picchioni, F.; Agarwal, U. S.; Wouters, D.; Loos, D.; Lemstra, P. J. *Macromol. Rapid Commun.* **2006**, *27*, 1073–1078.
(57) Doi, M.; Edwards, S. F. *J. Chem. Soc., Faraday Trans. 2* **1978**, *74*, 560–570.
(58) Islam, M. F.; Alsayed, A. M.; Dogic, Z.; Zhang, J.; Lubensky, T. C.; Yodh, A. G. *Phys. Rev. Lett.* **2004**, *92*, 0883031–4.
(59) Shaffer, M. S. P.; Windle, A. H. *Macromolecules* **1999**, *32*, 6864–6866.
(60) Shaffer, M. S. P.; Fan, X.; Windle, A. H. *Carbon* **1998**, *36*, 1603–1612.
(61) Hilding, J.; Grulke, E. A.; Zhang, Z. G.; Lockwood, F. *J. Dispersion Sci. Technol.* **2003**, *24*, 1–41.
(62) Strano, M. S.; Moore, V. C.; Miller, M. K.; Allen, M. J.; Haroz, E. H.; Kittrell, C.; Hauge, R. H.; Smalley, R. E. *J. Nanosci. Nanotechnol.* **2003**, *3*, 81–86.
(63) Yang, Y.; Grulke, E.; Zhang, Z. G.; Wu, G. *J. App. Phys.* **2006**, *99*, 114307.
(64) Yang, Y.; Grulke, E. A.; Zhang, Z. G.; Wu, G. *J. Nanosci. Nanotechnol.* **2005**, *5*, 571–579.